Weierstraß–Institut
für Angewandte Analysis und Stochastik

im Forschungsverbund Berlin e.V.

Preprint ISSN 0946 – 8633

Relaxation Properties of a 1D Flow through a Porous Material without and with Adsorption

Bettina Albers, Krzysztof Wilmański[1]

submitted: 4th December 2001

[1] Weierstrass Institute
for Applied Analysis
and Stochastics
Mohrenstr. 39
D – 10117 Berlin
Germany
E-Mail: albers@wias-berlin.de

Preprint No. 707
Berlin 2001

2000 *Mathematics Subject Classification.* 76S05, 76E20, 74J05.

Key words and phrases. flows in porous media, stability of geophysical flows, linear waves.

Edited by
Weierstraß–Institut für Angewandte Analysis und Stochastik (WIAS)
Mohrenstraße 39
D — 10117 Berlin
Germany

Fax: + 49 30 2044975
E-Mail (X.400): c=de;a=d400-gw;p=WIAS-BERLIN;s=preprint
E-Mail (Internet): preprint@wias-berlin.de
World Wide Web: http://www.wias-berlin.de/

Abstract

In this paper we investigate relaxation properties of a 1D steady state flow in a porous medium which is linearly perturbed in flow direction. We consider two cases of relaxation: without adsorption and with adsorption. The fields are assumed to be a superposition of a stationary (nonuniform) solution and of infinitesimal disturbances in the form of a linear wave ansatz. We show that such flows are absolutely stable with respect to longitudinal disturbances. It means that a smaller real part of the exponent in this ansatz yields a faster relaxation of the perturbation and the flow recovers faster the equilibrium. We solve numerically the eigenvalue problem for the first step field equations using a finite difference scheme and compare the results for the perturbation without mass exchange with the analytical solution. Calculations demonstrate the range of permeability coefficients with the fastest relaxation and the fastest convergence of numerical solutions.

1 Introduction

The main aim of this research is to investigate the stability of flows within the adsorption/diffusion model for porous materials as shown in Section 5.2.1 and introduced in [1] (see: [2] for a short english presentation). In the present work we limit our attention to the analysis of a 1D flow with a longitudinal disturbance.

In general flow instabilities arise due to at least two competing mechanisms – destabilizing, and stabilizing the flow. Conceivable are problems like a kinematic nonlinearity working against viscosity or gravity competing with a temperature gradient. In the case of our model for multicomponent systems, where a fluid flows through channels of a skeleton, a kinematic nonlinearity acts against the permeability (diffusion) of the medium. Adsorption processes contribute in a nonlinear way to field equations, and influence stability properties.

Two permeabilities of completely different nature enter the model: the permeability coefficient π, and the surface permeability α. The first one enters field equations and reflects a bulk property of the material. It describes the effective resistance of the skeleton to the flow of the fluid (due to a microgeometry of channels, due to the true viscosity of the fluid, etc.). The other permeability coefficient, the surface resistance α, enters the model through the boundary conditions of the third type, and it accounts for properties of the surface. This is one of the material parameters which determine the fluid velocity. Consequently these two important parameters of the model control two competing mechanisms responsible for the stability of the flow. The general aim of the analysis is to find regions of stability in the space spanned by these two parameters.

For this analysis the flow was split in a base flow and a superposed small perturbation in flow direction.

Numerical results show that the base flow for this type of perturbation is stable for any choice of the two model parameters. To observe instability regions it is necessary to superpose on the one dimensional base flow a perturbation perpendicular to the base flow. This analysis will be shown in a forthcoming paper. However longitudinal disturbances have an important practical bearing from the point of view of a sensitivity of the model on changes of the permeability coefficients. Namely they determine the rate of relaxation of dynamical disturbances.

In order to confirm numerical results for the case without mass exchange we compare them with the analytical solution. It is worth mentioning that this is the only analytical solution which we were able to construct for this model.

2 The problem

We consider a simple 1D flow process in a two component porous medium. In the following sections we examine the same 1D flow with two different longitudinal disturbances: without adsorption and with adsorption. Seperately we investigate the special case of the ideal surface permeability $\alpha \to \infty$ because we can construct an analytical solution for this case. The flow common for all considerations satisfies the following set of equations

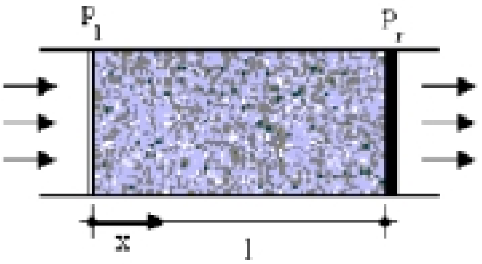

$$\frac{\partial \rho^F}{\partial t} + \frac{\partial \rho^F v^F}{\partial x} = 0, \tag{1}$$

$$\rho^F \left(\frac{\partial v^F}{\partial t} + v^F \frac{\partial v^F}{\partial x} \right) = -\frac{\partial p^F}{\partial x} - \pi v^F,$$

which are the mass balance of the fluid and the momentum balance of the fluid, respectively. Here, ρ^F is the mass density of the fluid component, v^F is the fluid velocity in x-direction, and π is the bulk permeability coefficient. The partial pressure in the fluid p^F is given by the following constitutive relation

$$p^F = \overset{0}{p} + \kappa \overset{1}{\rho}, \tag{2}$$

where $\overset{0}{p}$ is the fluid pressure in the base flow which depends on the chosen boundary conditions, $\overset{1}{\rho}$ is a small perturbation of the mass density of the fluid phase, and κ

denotes the compressibility coefficient. It is assumed that a deformed skeleton does not contribute to a dynamical disturbance. In addition the coupling to a changing porosity has been neglected because this contribution is of the higher order.

We consider the following boundary conditions

$$\begin{aligned} -\rho^F v^F\Big|_{x=0} &= \alpha\left[p^F\Big|_{x=0} - n_E p_l\right], \\ \rho^F v^F\Big|_{x=l} &= \alpha\left[p^F\Big|_{x=l} - n_E p_r\right], \end{aligned} \tag{3}$$

which are of third type and express the fact that the flow through the boundary of the body depends on the pressure difference of the partial pressure in the fluid $\left(p^F\right)$ and the external pressure which works on the fluid (on the left hand side p_l and on the right hand side p_r) as well as on the permeability of the surface which is denoted by α. n_E denotes a constant porosity.

3 Base flow

In the analysis we use a regular perturbation method restricted to zeroth and first order contributions. This means that we expect the fields to be a superposition of the base solution (indicated by 0) and a small perturbation in flow direction (indicated by 1)

$$\rho^F(x,t) = \overset{0}{\rho}(x) + \overset{1}{\rho}(x,t), \quad v^F(x,t) = \overset{0}{v}(x) + \overset{1}{v}(x,t), \quad 0 \leq x \leq l. \tag{4}$$

In order to be able to compare a numerical result with an analytical one for simplicity we assume the base flow to be isochoric. This means that in the zeroth step of perturbation the mass density is constant

$$\overset{0}{\rho} = \text{const} = \rho_0^F. \tag{5}$$

This simplification is supported by all calculations which we performed in earlier papers on porous media. Bearing $(1)_1$ for the zeroth step in mind we obtain that also the fluid velocity is constant

$$\overset{0}{v} = \text{const.} \tag{6}$$

Equation $(1)_2$ allows us to calculate a formal solution for the partial pressure in the fluid in the zeroth step

$$\frac{\partial \overset{0}{p}}{\partial x} = -\pi \overset{0}{v} \quad \Longrightarrow \quad \overset{0}{p} = -\pi \overset{0}{v} x + C, \tag{7}$$

where C is an integration constant which can be determined with the boundary condition on the left hand side of the system ($x = 0$)

$$-\rho_0^F \overset{0}{v} = \alpha\left[p^F\Big|_{x=0} - n_E p_l\right], \tag{8}$$

so that we obtain

$$\overset{0}{p} = -\pi \overset{0}{v} x + n_E p_l - \frac{\rho_0^F \overset{0}{v}}{\alpha}. \tag{9}$$

From the second boundary condition for $x = l$ we have

$$\rho_0^F \overset{0}{v} = \alpha \left[\left. p^F \right|_{x=l} - n_E p_r \right], \tag{10}$$

and the constant velocity of the zeroth step follows in the form

$$\overset{0}{v} = \frac{\alpha p_d}{2\rho_0^F + \alpha \pi l}, \qquad p_d := n_E \left(p_l - p_r \right). \tag{11}$$

In a more convenient form for further investigations (11) and (9) read

$$\overset{0}{v} = f \frac{p_d}{\pi l}, \quad \overset{0}{p} = n_E p_l - f p_d \frac{x}{l} - \frac{p_d}{2 + \frac{\alpha \pi l}{\rho_0^F}}, \qquad f := \frac{\frac{\alpha \pi l}{\rho_0^F}}{2 + \frac{\alpha \pi l}{\rho_0^F}}, \quad f \in [0, 1]. \tag{12}$$

4 Analytical approach

4.1 General solution for the first step

Let us remind that $\overset{0}{\rho}$ =const. so that also $\overset{0}{v}$ =const. We proceed to the first step of perturbation.

The perturbations in the first step are expressed in terms of the following simple wave ansatz

$$\overset{1}{\rho} = \bar{\rho}(x) \mathrm{e}^{\omega t}, \quad \overset{1}{v} = \bar{v}(x) \mathrm{e}^{\omega t}, \tag{13}$$

where $\bar{\rho}(x)$ and $\bar{v}(x)$ are the amplitudes of the disturbances and ω is the frequency, possibly complex.

Using this ansatz and keeping in mind the constitutive relation $\overset{1}{p} = \kappa \overset{1}{\rho}$ we get the following first order equations

$$\begin{aligned} &\omega \bar{\rho} + \rho_0^F \frac{\partial \bar{v}}{\partial x} + \overset{0}{v} \frac{\partial \bar{\rho}}{\partial x} = 0, \\ &\omega \bar{v} + \overset{0}{v} \frac{\partial \bar{v}}{\partial x} + \frac{\kappa}{\rho_0^F} \frac{\partial \bar{\rho}}{\partial x} + \frac{\pi}{\rho_0^F} \bar{v} = 0. \end{aligned} \tag{14}$$

The first step boundary conditions read

$$\begin{aligned} x = 0: &\quad -\rho_0^F \left. \bar{v} \right|_{x=0} = \left(\alpha\kappa + \overset{0}{v} \right) \left. \bar{\rho} \right|_{x=0}, \\ x = l: &\quad \rho_0^F \left. \bar{v} \right|_{x=l} = \left(\alpha\kappa - \overset{0}{v} \right) \left. \bar{\rho} \right|_{x=l}, \end{aligned} \qquad \overset{0}{v} = f \frac{p_d}{\pi l}. \tag{15}$$

From the governing set of equations (14) we can eliminate one field, say $\bar{v}$, so that we are left with an equation of the following form

$$\mathsf{a}\frac{\partial^2 \bar{\rho}}{\partial x^2} + \mathsf{b}\frac{\partial \bar{\rho}}{\partial x} + \mathsf{c}\bar{\rho} = 0, \tag{16}$$

with

$$\mathsf{a} = -\overset{0}{v}{}^2 + \kappa, \quad \mathsf{b} = -\overset{0}{v}\left(2\omega + \frac{\pi}{\rho_0^F}\right), \quad \mathsf{c} = -\omega\left(\omega + \frac{\pi}{\rho_0^F}\right), \tag{17}$$

whose solution is

$$\bar{\rho} = \mathsf{A}\mathrm{e}^{r_1 x} + \mathsf{B}\mathrm{e}^{r_2 x}, \qquad r_{1,2} = -\frac{1}{2}\frac{\mathsf{b} \mp \sqrt{\mathsf{b}^2 - 4\mathsf{ac}}}{\mathsf{a}}. \tag{18}$$

The boundary conditions (15) connect first step mass density and first step velocity. Namely

$$x = 0: \quad \left.\bar{\rho}\right|_{x=0} = -\frac{\rho_0^F}{\alpha\kappa + \overset{0}{v}}\left.\bar{v}\right|_{x=0}, \qquad x = l: \quad \left.\bar{\rho}\right|_{x=l} = \frac{\rho_0^F}{\alpha\kappa - \overset{0}{v}}\left.\bar{v}\right|_{x=l}. \tag{19}$$

Hence, in order to exploit them we also need the solution for the velocity which we get by integrating $(14)_1$ and inserting the solution (18)

$$\bar{v} + \underbrace{\mathsf{C}}_{\equiv 0} = -\frac{1}{\rho_0^F}\left[\omega\left(\frac{\mathsf{A}}{r_1}\mathrm{e}^{r_1 x} + \frac{\mathsf{B}}{r_2}\mathrm{e}^{r_2 x}\right) + \overset{0}{v}\left(\mathsf{A}\mathrm{e}^{r_1 x} + \mathsf{B}\mathrm{e}^{r_2 x}\right)\right]. \tag{20}$$

The additional integration constant can be easily proven to be identically zero. By insertion of the solutions in the boundary condition for $x = 0$ we obtain

$$\mathsf{B} = \frac{\alpha\kappa - \frac{\omega}{r_1}}{\frac{\omega}{r_2} - \alpha\kappa}\mathsf{A}. \tag{21}$$

Doing the same with the second condition for $x = l$ and using (21) we get for $\mathsf{A} \neq 0$

$$\begin{aligned} \mathrm{e}^{(r_1 - r_2)l} &= \frac{\alpha\kappa - \frac{\omega}{r_1}}{\alpha\kappa + \frac{\omega}{r_1}}\frac{\alpha\kappa + \frac{\omega}{r_2}}{\alpha\kappa - \frac{\omega}{r_2}} \\ \Leftrightarrow \quad \exp\left(l\frac{\sqrt{\mathsf{b}^2 - 4\mathsf{ac}}}{\mathsf{a}}\right) &= \frac{(\alpha\kappa\mathsf{b})^2 - \left(\alpha\kappa\sqrt{\mathsf{b}^2 - 4\mathsf{ac}} - 2\omega\mathsf{a}\right)^2}{(\alpha\kappa\mathsf{b})^2 - \left(\alpha\kappa\sqrt{\mathsf{b}^2 - 4\mathsf{ac}} + 2\omega\mathsf{a}\right)^2}. \end{aligned} \tag{22}$$

This equation for ω cannot be solved analytically in a general case. We demonstrate the solution for a particular case in the next section.

4.2 Surface permeability $\alpha \to \infty$

In the case of simple Darcy models of porous materials it is assumed that permeable boundaries are ideal. This means that the surface permeability coefficient α tends to infinity and the boundary conditions (3) reduce to the following ones

$$p^F\Big|_{x=0} = n_E p_l, \qquad p^F\Big|_{x=l} = n_E p_r. \tag{23}$$

This assumption simplifies considerably the equation (22), and simultaneously demonstrates important features of relaxation processes in the model. We proceed to investigate this case. From the second equation (1) together with the above boundary conditons we obtain

$$\overset{0}{v} = \frac{p_d}{\pi l} \quad (f = 1 \text{ in } (12)), \qquad \overset{0}{p^F} = -\pi \overset{0}{v} x + n_E p_l. \tag{24}$$

The first step boundary conditions are

$$\begin{aligned} \overset{1}{p}\Big|_{x=0} &= 0 \quad \Rightarrow \quad \overset{1}{\rho}\Big|_{x=0} = 0, \quad \Rightarrow \quad \bar{\rho}\big|_{x=0} = 0, \\ \overset{1}{p}\Big|_{x=l} &= 0 \quad \Rightarrow \quad \overset{1}{\rho}\Big|_{x=l} = 0, \quad \Rightarrow \quad \bar{\rho}\big|_{x=l} = 0. \end{aligned} \tag{25}$$

The first of them yields for the constants A, B of the solution (18)

$$\mathsf{A} = -\mathsf{B} \quad \Rightarrow \quad \bar{\rho} = \mathsf{A}\left(\mathrm{e}^{r_1 x} - \mathrm{e}^{r_2 x}\right). \tag{26}$$

The second condition leads to the dispersion relation for ω. Namely

$$\mathrm{e}^{r_1 l} - \mathrm{e}^{r_2 l} = 0 \quad \Leftrightarrow \quad \exp\left(-\frac{\mathsf{b} l}{2\mathsf{a}}\right) \sinh \frac{l\sqrt{\mathsf{b}^2 - 4\mathsf{ac}}}{2\mathsf{a}} = 0. \tag{27}$$

Certainly this is the limit $\alpha \to \infty$ of relation (22). Let us mention that the formal limit $\alpha \to 0$ is identical with this for $\alpha \to \infty$. However this limit yields also a singularity in the base solution. Namely the velocity $\overset{0}{v}$ is not only constant but it is equal to zero, and the pressure must be constant. In fact it becomes equal to the algebraic average of external pressures. It means that we have jumps on both ends: $x = 0$, $x = l$. We shall see further that this creates certain artefacts in numerical calculations for small values of α.

The exponential part of the last equation cannot be equal to zero. Hence

$$\sin i \frac{l\sqrt{\mathsf{b}^2 - 4\mathsf{ac}}}{2\mathsf{a}} = 0, \tag{28}$$

and this yields

$$\frac{l\sqrt{\mathsf{b}^2 - 4\mathsf{ac}}}{2\mathsf{a}} = -in\Pi, \quad n \in \mathbb{Z}^0, \quad \Pi = 3.14... \tag{29}$$

For $n = 0$ we obtain the following solutions for ω

$$\omega_0^{+,-} = \frac{1}{2}\frac{-\pi \pm \pi\sqrt{1-\frac{\overset{0}{v}{}^{2}}{\kappa}}}{\rho_0^F} \approx \begin{cases} 0 \\ -\frac{\pi}{\rho_0^F} \end{cases} . \tag{30}$$

The approximation follows from the fact that $\sqrt{\kappa}$ is the speed of the P2 wave. This means that the fraction $\frac{\overset{0}{v}{}^{2}}{\kappa} \sim \mathcal{O}\left(10^{-6}\right)$ for typical geotechnical applications (see: [3] for the details of parameter analysis). Both these solutions are obviously real. The first one yields the trivial solution $\mathsf{A} = \mathsf{B} = 0$ because otherwise the base solution (time independent!) would not be unique. Consequently solely the second solution for ω can be chosen, and this corresponds to the relaxation by damping which follows the resistance to the diffusion.

For $n \geq 1$ we obtain the solution

$$\omega_n^{+,-} = \begin{cases} \frac{1}{2}\left[-\frac{\pi}{\rho_0^F} \pm \sqrt{\left(\frac{\pi}{\rho_0^F}\right)^2 - 4\frac{\kappa\Pi^2 n^2}{l^2}}\right] & \text{for} \quad \pi > 2\frac{n\Pi\rho_0^F}{l}\sqrt{\kappa}, \\ \\ \frac{1}{2}\left[-\frac{\pi}{\rho_0^F} \pm i\sqrt{4\frac{\kappa\Pi^2 n^2}{l^2} - \left(\frac{\pi}{\rho_0^F}\right)^2}\right] & \text{for} \quad \pi < 2\frac{n\Pi\rho_0^F}{l}\sqrt{\kappa}. \end{cases} \tag{31}$$

We have used here again the approximation $\frac{\overset{0}{v}{}^{2}}{\kappa} \ll 1$.

This yields the following relation for the bigger of two real parts of ω_n :

$$\mathrm{Re}\omega_n^{+} = \begin{cases} -\frac{\pi}{2\rho_0^F} & \text{for} \quad \pi < 2\frac{n\Pi\rho_0^F}{l}\sqrt{\kappa}, \\ -\frac{\pi}{2\rho_0^F} + \frac{1}{2}\sqrt{\left(\frac{\pi}{\rho_0^F}\right)^2 - 4\frac{\kappa\Pi^2 n^2}{l^2}} & \text{for} \quad \pi > 2\frac{n\Pi\rho_0^F}{l}\sqrt{\kappa}. \end{cases} \tag{32}$$

Clearly we have for any $n \geq 1$

$$\mathrm{Re}\omega_n^{+} \geq \mathrm{Re}\omega_{n+1}^{+}. \tag{33}$$

Hence the biggest real part of the exponent appears for $n = 1$. We obtain

$$\max_n \left\{\mathrm{Re}\omega_n^{+,-}\right\} = \begin{cases} -\frac{\pi}{2\rho_0^F} & \text{for} \quad \pi < 2\frac{\Pi\rho_0^F}{l}\sqrt{\kappa}, \\ -\frac{\pi}{2\rho_0^F} + \frac{1}{2}\sqrt{\left(\frac{\pi}{\rho_0^F}\right)^2 - 4\frac{\kappa\Pi^2}{l^2}} & \text{for} \quad \pi > 2\frac{\Pi\rho_0^F}{l}\sqrt{\kappa}. \end{cases} \tag{34}$$

The above results are illustrated by the following example:

Length of the body l	1m	Equilibrium porosity n_E	0.23
Compressibility κ	$2.25 \cdot 10^6\ \frac{\mathrm{m}^2}{\mathrm{s}^2}$	Initial mass density ρ_0^L	$2.3 \cdot 10^2\ \frac{\mathrm{kg}}{\mathrm{m}^3}$
Pressure left h.s. p_l	110kPa	Pressure right h.s. p_r	100kPa
Pressure difference working	on the fluid	$p_d = n_E\left(p_l - p_r\right)$	2.3kPa

Table 1: Typical model parameters for flow processes in soils

The data in the table are typical for geotechnical applications.

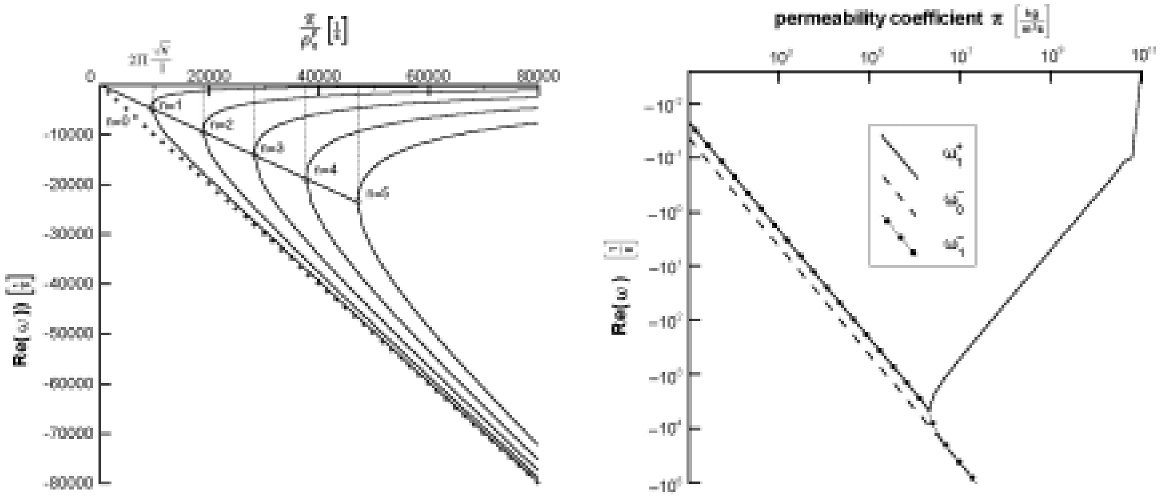

a)

b)

Fig. 1: Analytical solution for the flow without mass exchange

In Figure 1 we demonstrate the above results in two scales. In the left part a) we show the relations (30) and (32) in a linear scale for different n. As we see all relations for $\operatorname{Re}(\omega), n \geq 1$, contain the turning point $\pi_0 = 2\frac{n\Pi\rho_0^F}{l}\sqrt{\kappa}$ (indicated by small circles in Fig. 1a)) which divides the range of π into the part, where the solution of the dispersion relation (28) is complex (small π), and the part, where it is real (large π). The former means that the disturbance consists of the exponential relaxation, and vibrations.

It is clear that the biggest real part of ω appears for $n = 1$. This is shown in the right part b) of Figure 1 in the log-log scale. Such a scale is used in all figures for processes without mass exchange which appear further in this paper. The logarithmic scales lead to distortion of the curves for very small, and very large values of π. These distortions do not have any physical meaning. As we see further such a distortion appears also in numerical calculations.

4.3 Comments

We have learned from the above analytical solution that the relaxation properties do not change monotonously with the permeability π. They possess rather two different ranges. In the range of smaller values of π the relaxation is determined by a real part of the complex root, while for larger π this root does not possess an imaginary part. It means that the perturbation causes vibrations in the range of smaller π, whose frequencies cover the whole discrete spectrum (different values of n in (31)).

As we see further such a turning point appears for all finite values of α even though it is not so well defined as in the above case.

Simultaneously the position of the turning point is determinated by the compressibility coefficient of the fluid. We return to this property after the numerical analysis.

5 Numerical investigation

The relaxation properties of the 1D flow are numerically investigated for two cases: the first one: a perturbation without mass exchange where we distinguish between $\alpha = \infty$ and variable α, and the second one: with mass exchange for variable α.

5.1 Disturbance without mass exchange

5.1.1 Results

We solve the eigenvalue problem for ω numerically, using a second order finite difference scheme in a equidistant mesh (length of the body l divided into n parts of length h). The derivatives of disturbances are written as central differences $\left(\frac{\partial u}{\partial x} = \frac{u(x+h)-u(x-h)}{2h}\right)$ for inner mesh points, or as asymmetric ones for the first $\left(\frac{\partial u}{\partial x} = \frac{u(x+h)-u(x)}{h}\right)$, and the last point $\left(\frac{\partial u}{\partial x} = \frac{u(x)-u(x-h)}{h}\right)$. For this linear eigenvalue problem we obtain for both cases without mass exchange $2n$ eigenvalues ω_i (number of linear equations: $2\left(n+1\right)-2)$. The exponential form of the ansatz (13) yields that the base flow is stable if all real parts of ω_i are negative and unstable if at least one of the $2n$ real parts is positive. Consequently in the case of stable processes we prove numerically that the biggest real part of eigenvalues is negative. In the case of this value being positive the perturbance would increase and the exponential term would explode in time. The smaller this negative value the faster the flow tends to the steady state situation.

The results of the numerical investigation are given in Figs. 2 and 3 in log-log scale. However, in order to show the pecularity of the turning point, we also show the curve for $\alpha \to \infty$ in the log-linear scale (the small picture in Fig. 2 for $10^3 \leq \pi \leq 10^9$).

Let us begin with the special case $\alpha \to \infty$. We have checked that for $\alpha > 10^{-2} \frac{\mathrm{s}}{\mathrm{m}}$ our numerical procedure becomes unstable. However the numerical results for smaller values of α converge regularly to the result for $\alpha = 10^{-2} \frac{\mathrm{s}}{\mathrm{m}}$ and, on the other hand, this result is identical with our analytical result of the previous section. This indicates that the behaviour for large α can be well approximated by this for $\alpha = 10^{-2} \frac{\mathrm{s}}{\mathrm{m}}$. For completeness we have checked this using a different numerical scheme for $\alpha \to \infty$, and the result is shown in Fig. 2. As seen in Fig. 3 where all numerical results for different α are presented, in the range $\alpha > 10^{-2} \frac{\mathrm{s}}{\mathrm{m}}$ the solution does not change considerably.

5.1.2 Discussion

From the above figures it is obvious that for any pair (α, π) the maximum real part of the eigenvalues remains negative which means that the steady state base flow is stable with respect to a longitudinal disturbance without mass exchange. However relaxation properties of such disturbances are quite different for different values of permeabilites π, and α.

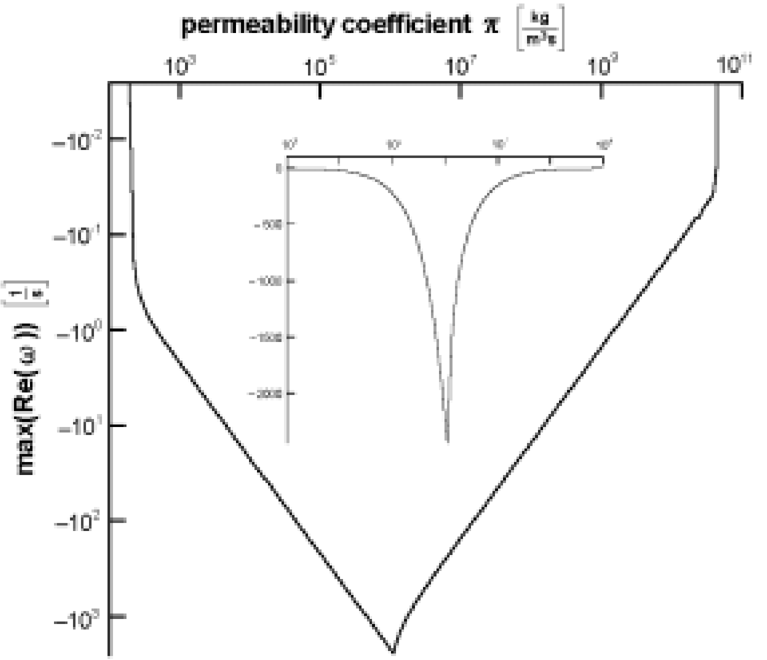

Fig. 2: Numerical result without mass exchange, $\alpha = \infty$

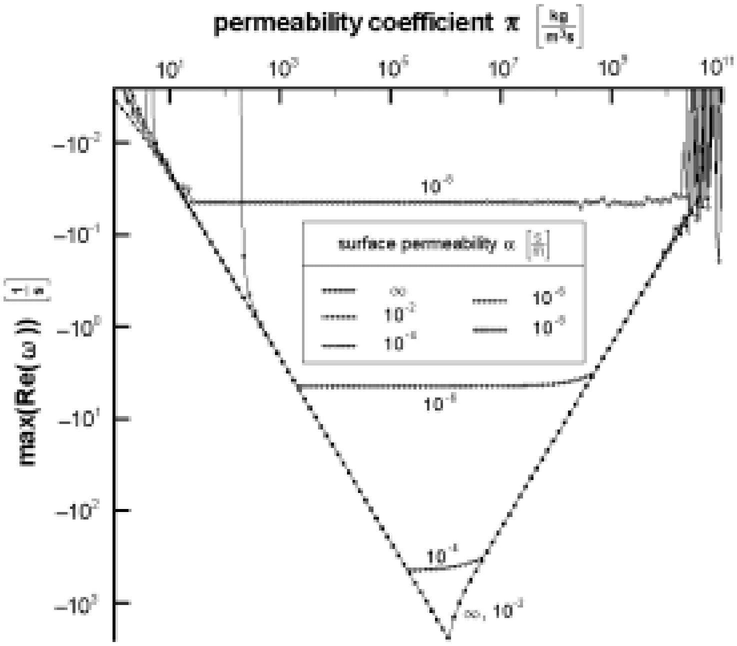

Fig. 3: Numerical result without mass exchange, variable α

First of all, for any choice of α, there exists a region of π in which eigenvalues are complex, i.e. disturbances lead to vibrations. This region of relatively small bulk permeability π becomes smaller for smaller α. For values of π bigger than this of the turning point the disturbance is only damped but the damping is smaller than this predicted by the resistance to the diffusion $\left(\text{i.e.} < \frac{\pi}{\rho_0^F}\right)$.

In general the damping is smallest (i.e. the relaxation is slowest) for large and small values of π. In fact it is almost constant in large ranges which are distorted in the figures by the logarithmic scale. Solely in the vicinity of the turning point the relaxation becomes considerably fast.

As we have already mentioned in Sec. 4.3. the position of the turning point is determined by the compressibility coefficient of the fluid. We demonstrate this property in Fig. 4 for $\alpha = 10^{-2}\frac{\mathrm{s}}{\mathrm{m}}$.

As we see the range in which the disturbance yields not only relaxation but also vibrations (small π) becomes smaller for smaller compressibility coefficient κ. Also the relaxation of the disturbances is slower for smaller compressibility coefficients.

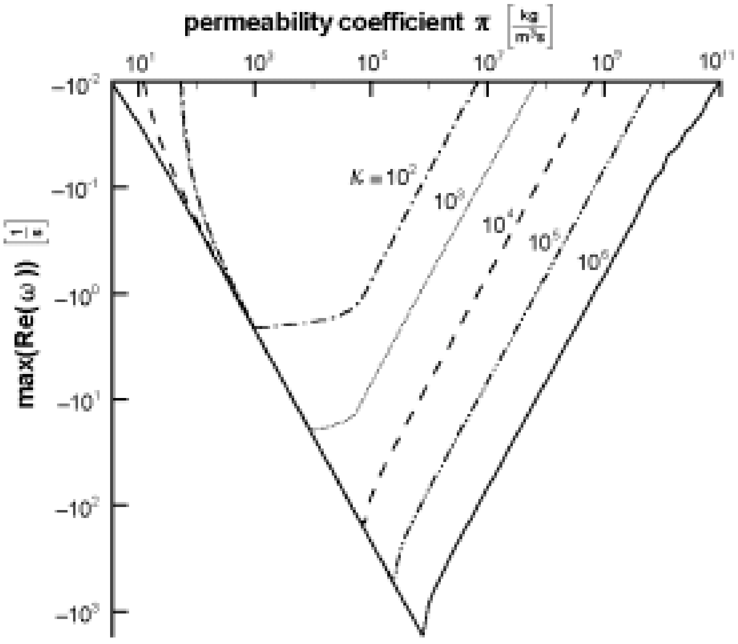

Fig. 4: Influence of the compressibility coefficient

5.2 Disturbance with mass exchange

5.2.1 Adsorption/diffusion model

We consider a process of physical adsorption in a porous medium. A fluid-adsorbate mixture flows through the channels of the skeleton. In principle the model (see: B. Albers [1] and [2]) takes into account three components: the skeleton, the fluid and an adsorbate which flows with the same velocity as the fluid through channels of the skeleton until it settles down on the inner surface of the porous body. As before we neglect the dynamics of the skeleton.

Mass balances

Then the mass balance equation for the liquid and the concentration balance have the following form

$$\begin{aligned} \frac{\partial \rho^L}{\partial t} + \frac{\partial \rho^L v^F}{\partial x} &= \hat{\rho}^A, \\ \rho^L \left(\frac{\partial c}{\partial t} + v^F \frac{\partial c}{\partial x} \right) &= (1-c)\, \hat{\rho}^A, \end{aligned} \tag{35}$$

where ρ^L is the mass density of the liquid phases, i.e. the sum of the mass densities of the fluid and the adsorbate, and c denotes the concentration of the adsorbate in the fluid component. The common velocity of fluid and adsorbate is denoted by v^F.

The concentration balance $(35)_2$ follows from the mass balance for the adsorbate. Finally, the intensity of the mass source is denoted by $\hat{\rho}^A$.

Mass source

The latter is given by the relation

$$\hat{\rho}^A = -\frac{m^A}{V}\frac{d\left(\xi\, f_{int}\right)}{dt} = -\frac{m^A}{V}\left(f_{int}\frac{d\xi}{dt} + \xi\frac{d\, f_{int}}{dt}\right), \tag{36}$$

whose derivation is based on the classical LANGMUIR adsorption theory utilizing the notions of *occupied* (ξ) and *bare* ($1-\xi$) *sites* (e.g. see [4]) on the internal surface f_{int} of the solid. V is the representative elementary volume REV and m_A denotes the mass of adsorbate per unit area of the internal surface .

The first contribution on the right-hand side of (36) describes changes in time of the fraction of occupied sites. It is specified by the Langmuir evolution equation which can be written in the form

$$\frac{\partial \xi}{\partial t} = \left[\frac{cp^L}{p_0}\left(1-\xi\right) - \xi\right]\frac{1}{\tau_{ad}}, \tag{37}$$

where p^L denotes the partial pressure in the liquid (fluid and adsorbate together), p_0 is a Langmuir reference pressure and τ_{ad} is the characteristic time of adsorption. In the static case the well-known *Langmuir isotherm of occupied sites* follows from this relation

$$\xi_L = \frac{\frac{cp^L}{p_0}}{1+\frac{cp^L}{p_0}}, \tag{38}$$

where according to Dalton´s law for small concentrations of the adsorbate it is assumed that the partial pressure of the adsorbate $p^A \cong cp^L$.

The other part of (36) describes the change of the internal surface. We assume this change to be coupled with the relaxation of porosity. But due to the assumption of constant porosity it disappears from the equations in this work. This is justified by results of our earlier works that the Langmuir part of the mass source is much more important than the part connected with changes of the porosity.

Finally we obtain the following form of the mass source

$$\hat{\rho}^A = -\rho^A_{ad}\left\{\left[\frac{cp^L}{p_0}\left(1-\xi\right) - \xi\right]\frac{1}{\tau_{ad}}\right\}, \tag{39}$$

where and $\rho^A_{ad} := \frac{m^A f_{int}}{V}$.

Momentum balance

Due to the same velocity of fluid and adsorbate we need only one momentum balance common for these both components. We have

$$\rho^L \left[\frac{\partial v^F}{\partial t} + v^F \frac{\partial v^F}{\partial x} \right] = -\frac{\partial p^L}{\partial x} - \pi v^F.$$

Also here, a linear constitutive relation for the pressure in the liquid phase p^L

$$p^L = \overset{0}{p} + \kappa \overset{1}{\rho}, \tag{40}$$

is used and the permeability coefficient π and the compressibility coefficient κ are assumed to be constant.

5.2.2 Governing equations

Bearing the above considerations in mind we have in 1D to examine the behaviour of the flow described by the following set of equations

$$\begin{aligned}
&\frac{\partial \rho^L}{\partial t} + \rho^L \frac{\partial v^F}{\partial x} + v^F \frac{\partial \rho^L}{\partial x} = -\frac{\rho^A_{ad}}{\tau_{ad}} \left[\frac{c p^L}{p_0} (1-\xi) - \xi \right], \\
&\rho^L \left[\frac{\partial c}{\partial t} + v^F \frac{\partial c}{\partial x} \right] = -(1-c) \frac{\rho^A_{ad}}{\tau_{ad}} \left[\frac{c p^L}{p_0} (1-\xi) - \xi \right], \\
&\frac{\partial \xi}{\partial t} = \frac{1}{\tau_{ad}} \left[\frac{c p^L}{p_0} (1-\xi) - \xi \right], \\
&\rho^L \left[\frac{\partial v^F}{\partial t} + v^F \frac{\partial v^F}{\partial x} \right] = -\frac{\partial p^L}{\partial x} - \pi v^F,
\end{aligned} \tag{41}$$

rather than the set (1) for flows without adsorption.

5.2.3 Perturbation

In comparison to the case without mass exchange we have two additional fields which are subject to the regular perturbation, again restricted to zeroth and first order contributions

$$\begin{gathered}
\rho^L(x,t) = \overset{0}{\rho}(x) + \overset{1}{\rho}(x,t), \quad c(x,t) = \overset{0}{c}(x) + \overset{1}{c}(x,t), \\
\xi(x,t) = \overset{0}{\xi}(x) + \overset{1}{\xi}(x,t), \quad v^F(x,t) = \overset{0}{v}(x) + \overset{1}{v}(x,t), \quad 0 \le x \le l.
\end{gathered} \tag{42}$$

Zeroth step of perturbation

Also for this case we assume the base solution for the mass density $\overset{0}{\rho}$ to be constant. Again it follows that the velocity $\overset{0}{v}$ is constant (compare (12)). For the missing base solutions $\overset{0}{c}$ and $\overset{0}{\xi}$ we obtain the following equations (the zeroth step of perturbation)

concentration balance

$$\overset{0}{\rho}\overset{0}{v}\frac{\partial \overset{0}{c}}{\partial x} = -\left(1-\overset{0}{c}\right)\frac{\rho^A_{ad}}{\tau_{ad}}\left[\frac{\overset{0}{c}\overset{0}{p}}{p_0}\left(1-\overset{0}{\xi}\right)-\overset{0}{\xi}\right], \tag{43}$$

evolution equation for fraction of occupied sites

$$0 = \frac{\overset{0}{c}\overset{0}{p}}{p_0}\left(1-\overset{0}{\xi}\right)-\overset{0}{\xi}. \tag{44}$$

where $\overset{0}{p}$ is given by the relation (12). From (44) we obtain the relation for the Langmuir adsorption isotherm

$$\overset{0}{\xi} = \frac{\frac{\overset{0}{c}\overset{0}{p}^L}{p_0}}{1+\frac{\overset{0}{c}\overset{0}{p}^L}{p_0}}, \tag{45}$$

which, of course, varies with x due to the varying pressure $\overset{0}{p}$. Simultaneously from (43) we have

$$\overset{0}{c} = \text{const.} = c_0, \tag{46}$$

where c_0 denotes the initial concentration of the adsorbate in the fluid.

First step of perturbation

For the first step of perturbation we obtain the following set of equations

$$\begin{aligned}
&\frac{\partial \overset{1}{\rho}}{\partial t}+\overset{0}{\rho}\frac{\partial \overset{1}{v}}{\partial x}+\overset{0}{v}\frac{\partial \overset{1}{\rho}}{\partial x} = \overset{1}{\hat{\rho}}{}^A,\\
&\overset{0}{\rho}\left(\frac{\partial \overset{1}{c}}{\partial t}+\overset{0}{v}\frac{\partial \overset{1}{c}}{\partial x}\right) = \left(1-c_0\right)\overset{1}{\hat{\rho}}{}^A-\overset{1}{c}\frac{\rho^A_{ad}}{\tau_{ad}}\left[\frac{c_0\overset{0}{p}}{p_0}\left(1-\overset{0}{\xi}\right)-\overset{0}{\xi}\right],\\
&\frac{\partial \overset{1}{\xi}}{\partial t} = \left[\left(1-\overset{0}{\xi}\right)\frac{c_0\kappa\overset{1}{\rho}+\overset{1}{c}\overset{0}{p}}{p_0}-c_0\overset{1}{\xi}\frac{\overset{0}{p}}{p_0}-\overset{1}{\xi}\right]\frac{1}{\tau_{ad}},\\
&\overset{0}{\rho}\left(\frac{\partial \overset{1}{v}}{\partial t}+\overset{0}{v}\frac{\partial \overset{1}{v}}{\partial x}\right) = -\kappa\frac{\partial \overset{1}{\rho}}{\partial x}-\pi\overset{1}{v},
\end{aligned} \tag{47}$$

with

$$\overset{1}{\hat{\rho}}{}^A = -\frac{\rho^A_{ad}}{\tau_{ad}}\left[\frac{c_0\kappa\overset{1}{\rho}+\overset{1}{c}\overset{0}{p}}{p_0}\left(1-\overset{0}{\xi}\right)-\overset{1}{\xi}\left(1+\frac{c_0\overset{0}{p}}{p_0}\right)\right]. \tag{48}$$

The boundary conditions for this step have again the form

$$\begin{aligned} x=0: &\quad -\rho_0^F\,\bar{v}\big|_{x=0} = \left(\alpha\kappa + \overset{0}{v}\right)\bar{\rho}\big|_{x=0}\,,\\ x=l: &\quad \rho_0^F\,\bar{v}\big|_{x=l} = \left(\alpha\kappa - \overset{0}{v}\right)\bar{\rho}\big|_{x=l}\,. \end{aligned} \tag{49}$$

5.2.4 Wave ansatz

Again we assume for the perturbations the wave ansatz

$$\overset{1}{\rho} = \bar{\rho}\,(x)\,\mathrm{e}^{\omega t}, \quad \overset{1}{c} = \bar{c}\,(x)\,\mathrm{e}^{\omega t}, \quad \overset{1}{\xi} = \bar{\xi}\,(x)\,\mathrm{e}^{\omega t}, \quad \overset{1}{v} = \bar{v}\,(x)\,\mathrm{e}^{\omega t}, \tag{50}$$

by means of which we obtain the set of ordinary equations for the first step

$$\begin{aligned} &\omega\bar{\rho} + \overset{0}{\rho}\frac{\partial\bar{v}_x}{\partial x} + \overset{0}{v}\frac{\partial\bar{\rho}}{\partial x} = -\frac{\rho^A_{ad}}{\tau_{ad}}\left[\frac{c_0\kappa\bar{\rho} + \bar{c}\overset{0}{p}}{p_0}\left(1-\overset{0}{\xi}\right) - \bar{\xi}\left(1+\frac{c_0\overset{0}{p}}{p_0}\right)\right],\\ &\overset{0}{\rho}\left(\omega\bar{c} + \overset{0}{v}_x\frac{\partial\bar{c}}{\partial x}\right) = -\left(1-c_0\right)\frac{\rho^A_{ad}}{\tau_{ad}}\left[\frac{c_0\kappa\bar{\rho} + \bar{c}\overset{0}{p}}{p_0}\left(1-\overset{0}{\xi}\right) - \right.\\ &\qquad\qquad \left. -\bar{\xi}\left(1+\frac{c_0\overset{0}{p}}{p_0}\right)\right] - \bar{c}\frac{\rho^A_{ad}}{\tau_{ad}}\left[\frac{c_0\overset{0}{p}}{p_0}\left(1-\overset{0}{\xi}\right) - \overset{0}{\xi}\right],\\ &\omega\bar{\xi} = \left[\frac{c_0\kappa\bar{\rho} + \bar{c}\overset{0}{p}}{p_0}\left(1-\overset{0}{\xi}\right) - \bar{\xi}\left(1+\frac{c_0\overset{0}{p}}{p_0}\right)\right]\frac{1}{\tau_{ad}},\\ &\overset{0}{\rho}\left(\omega\bar{v} + \overset{0}{v}\frac{\partial\bar{v}}{\partial x}\right) = -\kappa\frac{\partial\bar{\rho}}{\partial x} - \pi\bar{v}. \end{aligned} \tag{51}$$

This means that we have to analyse the following relation

$$\left(\omega\mathsf{I} + \mathfrak{A}\right)\mathbf{u} + \mathfrak{B}\mathbf{u}' = 0, \tag{52}$$

with

$$\begin{aligned} \mathbf{u} &:= \left(\bar{\rho}, \bar{c}, \bar{\xi}, \bar{v}\right)^T, \quad \mathbf{u}' := \left(\frac{\partial\bar{\rho}}{\partial x}, \frac{\partial\bar{c}}{\partial x}, \frac{\partial\bar{\xi}}{\partial x}, \frac{\partial\bar{v}}{\partial x}\right)^T,\\ \mathsf{I} &:= \begin{pmatrix} 1 & 0 & 0 & 0\\ 0 & 1 & 0 & 0\\ 0 & 0 & 1 & 0\\ 0 & 0 & 0 & 1 \end{pmatrix}, \quad \mathfrak{B} := \begin{pmatrix} \overset{0}{v} & 0 & 0 & \overset{0}{\rho}\\ 0 & \overset{0}{v} & 0 & 0\\ 0 & 0 & 0 & 0\\ \dfrac{\kappa}{\overset{0}{\rho}} & 0 & 0 & \overset{0}{v} \end{pmatrix}, \end{aligned} \tag{53}$$

$$\mathfrak{A} := \begin{pmatrix} \frac{\rho^A_{ad}}{\tau_{ad}}\frac{c_0\kappa}{p_0}\left(1-\overset{0}{\xi}\right) & \frac{\rho^A_{ad}}{\tau_{ad}}\frac{\overset{0}{p}}{p_0}\left(1-\overset{0}{\xi}\right) & -\frac{\rho^A_{ad}}{\tau_{ad}}\left(1+\frac{c_0\overset{0}{p}}{p_0}\right) & 0 \\ \frac{1-c_0}{\overset{0}{\rho}}\frac{\rho^A_{ad}}{\tau_{ad}}\frac{c_0\kappa}{p_0}\left(1-\overset{0}{\xi}\right) & \begin{array}{c} \frac{1-c_0}{\overset{0}{\rho}}\frac{\rho^A_{ad}}{\tau_{ad}}\frac{\overset{0}{p}}{p_0}\left(1-\overset{0}{\xi}\right)+ \\ +\frac{1}{\overset{0}{\rho}}\frac{\rho^A_{ad}}{\tau_{ad}}\left[\frac{c_0\overset{0}{p}}{p_0}\left(1-\overset{0}{\xi}\right)-\overset{0}{\xi}\right] \end{array} & -\frac{1-c_0}{\overset{0}{\rho}}\frac{\rho^A_{ad}}{\tau_{ad}}\left(1+\frac{c_0\overset{0}{p}}{p_0}\right) & 0 \\ -\frac{c_0\kappa}{p_0}\left(1-\overset{0}{\xi}\right)\frac{1}{\tau_{ad}} & -\frac{\overset{0}{p}}{p_0}\left(1-\overset{0}{\xi}\right)\frac{1}{\tau_{ad}} & \left(1+\frac{c_0\overset{0}{p}}{p_0}\right)\frac{1}{\tau_{ad}} & 0 \\ 0 & 0 & 0 & \frac{\pi}{\overset{0}{\rho}} \end{pmatrix}$$

In the calculations we use in addition to the data of Table 1 the following quantities which enter the model due to the adsorption process:

Initial concentration c_0	10^{-3}
Langmuir pressure p_0	10 kPa
Charact. time of adsorp. τ_{ad}	1s
mass density of adsorbate on internal surface ρ^A_{ad}	40 $\frac{\text{kg}}{\text{m}^3}$

Table 2: Additional model parameters for adsorption processes in soils

Again we use a second order finite difference scheme as described in 5.1.1. in order to solve numerically the above eigenvalue problem. This leads to $4n+2$ eigenvalues ω_i (number of linear equations: $4(n+1)-2$).

Results are shown in the following Figure 5.

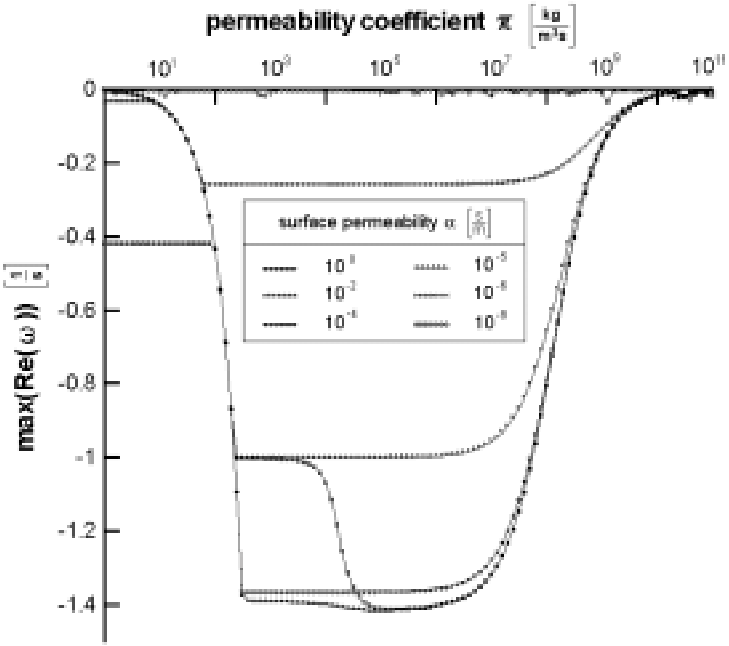

Fig. 5: Numerical result with mass exchange

5.2.5 Discussion

Similarly to the case without mass exchange the base steady state flow is stable with respect to a longitudinal disturbance with mass exchange for any choice of parameters (α, π).

However the relaxation of disturbances differs considerably from the previous case. Comparison of Fig. 3 and Fig. 5 shows that the mass exchange slows down the relaxation even a few orders of magnitude. This effect is related to the characteristic time of adsorption τ_{ad}. Little can be said about its experimental values for porous materials because most experiments are conducted in quasistatic conditions. In Fig. 6 we show the influence of τ_{ad} on the relaxation properties for $\alpha = 10^{-4} \frac{\mathrm{s}}{\mathrm{m}}$.

As expected disturbances relax faster for smaller characteristic times τ_{ad} but even for a very short time of adsorption $\tau_{ad} = 10^{-5}$s this relaxation is considerably longer than entirely without mass exchange.

In addition the range of vibrations (small values of π) is separated from a pure damping (large values of π) by more plateaus rather than a turning point, and a small single plateau appearing in perturbations without mass exchange.

Moreover due to the higher number of fields the different behaviour of relaxation appears in at least three different domains of π rather than two – characteristic for the previous case. This is caused by the activation of different eigenvalues corresponding to different mechanisms of the process.

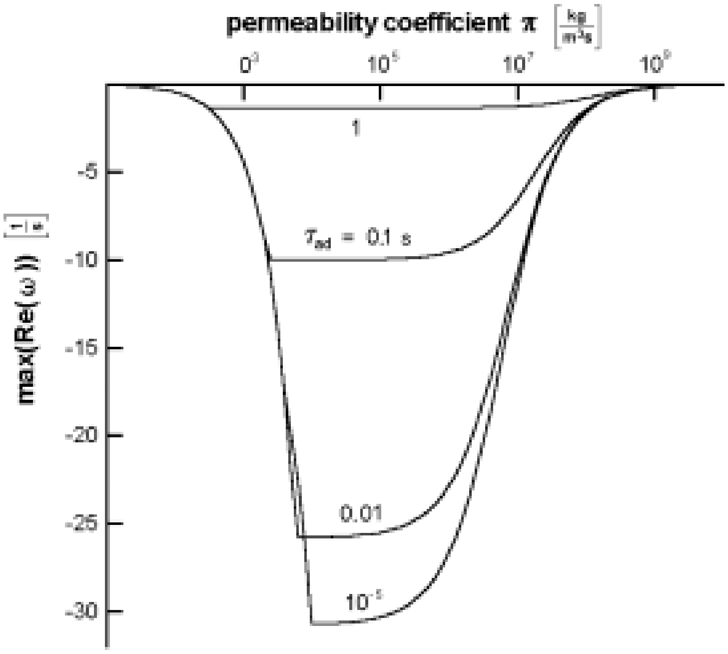

Fig. 6: Influence of the characteristic time of adsorption

6 Conclusions

We have shown that the 1D steady state flow through the porous material is stable with respect to a linear longitudinal disturbance without and with mass exchange in the whole range of control permeability parameters π, and α.

However the relaxation of such disturbancs is not determined solely by the diffusion. In all cases it is slower than the exponent $\frac{\pi}{\rho_0^F}$ characteristic for the diffusion. This results primarily from the compressibility of the fluid as we have indicated in the paper.

In addition in the range of small values of the permeability π there appear vibrations. This may indicate the existence of instabilities in the case of transversal disturbances. The latter problem shall be presented in a seperate paper.

Let us mention finally that the range of very large permeabilities π corresponds to relaxation considerably influenced by the compressibility and this is again much slower than expected from diffusion processes. As seen from the relation (34) the dependence on the compressibility is coupled to the length l. In the limit of the infinite medium $l \to \infty$ the influence of the compressibility vanishes entirely and the system possesses only a damped solution corresponding to the dashed line in Fig. 1a). Otherwise there exists always a region with vibrations. This property appears not only in the case solved analytically but also for all other cases, and follows from the hyperbolicity of the system. Namely if the damping $\frac{\pi}{\rho_0^F}$ is small enough the relaxation of the system is influenced by waves propagating between both ends of the system.

References

[1] ALBERS, B.: Makroskopische Beschreibung von Adsorptions-Diffusions-Vorgängen in porösen Körpern, PhD thesis TU Berlin, Logos-Verlag, Berlin, 2000.

[2] ALBERS, B.: Coupling of Adsorption and Diffusion in Porous and Granular Materials. A 1-D Example of the Boundary Value Problem, *Arch.Appl.Mech.,* **70** 7, 519-531, 2000.

[3] ALBERS, B.: Dependence of Adsorption/Diffusion Processes in Porous Media on Bulk and Surface Permeabilities, *Arch.Mech.*, **53**, 4–5, 289-306, 2001.

[4] GREGG, S. J.; SING, K. S. W.: Adsorption, Surface Area and Porosity, *Academic Press*, London, 1982.

[5] Wilmański, K.: Porous Media at Finite Strains. The New Model with the Balance Equation for Porosity, *Arch. Mech.*, **48**, 4, 591-628, 1996.

[6] Wilmański, K.: A Thermodynamic Model of Compressible Porous Materials with the Balance Equation of Porosity, *Transport in Porous Media*, **32**, 21-47, 1998.